Analysis of Bending Fracture Propagation of Laminar Composite Materials Using Quasi-Molecular Dynamics

Youngsuk Kim* and Junyoung Park**

(*Received December 13, 1997*)

Recently, quasimolecular dynamics has been successfully used to simulate the deformation characteristics of actual size solid materials. In quasimolecular dynamics, which is an attempt to bridge the gap between atomistic and continuum simulations, molecules are aggregated into large units, called quasimolecules, to evaluate large scale material behavior. In this paper, a 2 -dimensional numerical simulation using quasimolecular dynamics has been performed to investigate laminar composite material fracture and crack propagation behavior in the uniform bending of laminar composite materials. We verified that laminar composite materials deform quite differently from the case of homogeneous materials under bending deformation

Key Words: Laminar Composite Material, Crack Propagation, Quasimolecular Dynamics

1. Introduction

Recently, a new approach has tried to simulate the fracture processing of materials at the microscopic level using molecular dynamics(MD). The MD deals with the interacting behavior among molecules in order to reveal fracture behavior (Decelis, et al. , 1983; Kitagawa, et al. , 1993). Nevertheless, material size that can be analysed using MD is limited because the material of actual size is composed of an infinite number of molecules. The, quasimolecular dynamics (QMD) approach proposed by Greenspan makes such an analysis possible, in that molecules are aggregated into large units, called virtual quasimolecules (Greenspan, 1986;, Greenspan, 1989). Investigations of QMD to industrial applications have been performed, with the exception bending simulation(Kim and Park, 1997).

The study of the fracture behavior of laminar composite materials is motivated by practical situations encountered in the aerospace industry, the hull structure of chemical tankers, and other fields in which these materials are used extensively(Maiti and Sinha, 1996; Suga, et al, 1989). The situation is critical when the crack or void induces serious damage, detectable or undetectable by visual inspection, that causes a reduction in the strength and stability of the structure.

In this paper, crack generation and propagation of laminar composite materials subjected to uniform bending is numerically simulated and discussed within the framework of Greenspan's QMD method. Moreover we verify that laminar composite materials deforms quite differently from homogeneous materials under uniform bending deformation(Kim and Park, 1997; Triantafyllidis, et al. , 1982; Kim and Park, 1998).

2. Basic Theory

Consider a rectangular Cu-plate which is 8×19.9186 cm as in Fig. 1. From the Lennoard -Jones potential function acting between two atoms r Å apart,

$$\Phi(r) = -\frac{1.398068\times 10^{-10}}{r^6} + \frac{1.55104\times 10^{-8}}{r^{12}} \quad (erg) \tag{1}$$

while the force F interacting between two copper atoms is derived as follows(Greenspan, 1986)

* Department of Mechanical Engineering, Kyungpook National University

** Graduate School, Department of Mechanical Engineering, Kyungpook National University

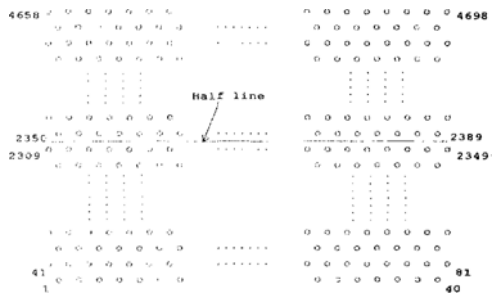

Fig. 1 The initial arrangement for the homogeneous material specimen.

$$F(r)=\frac{d\Phi}{dr}$$
$$=-\frac{8.38840\times10^{-2}}{r^{7}}+\frac{1.866125\times10}{r^{13}}(dyn) \quad (2)$$

in which r is measured in angstroms. Here we assume virtual quasimolecules are an aggregation of many molecules into larger units, and the equilibrium-distance between quasimolecules is 0.2cm. This means that each quasimolecule contains Cu-molecules of number of $N^{*}=6.47323\times10^{13}$. Therefore, its mass is $m=N^{*}*1.0542\times10^{-22}$ (g) $=6.824079\times10^{-9}$(g). Here the force function interacting between two quasimolecules is given by(Kim and Park, 1998)

$$F(R)=\frac{G}{R^{3}}+\frac{H}{R^{5}} \quad (3)$$

From the condition $F(0.2)=0$ and the energy conservation law, the force function acting between two quasimolecules is derived as follows

$$F(R)=-\frac{3.262974315}{R^{3}}+\frac{0.130518972}{R^{5}} \quad (4)$$

We now introduce a normalizing constant α such that at a distance 0.4 cm the force between the quasimolecules is small relative to their weight. If we define "small relative to weight" to mean 0.1% of the effect the weight, then we must have

$$\alpha\left|\frac{-3.262974315}{(0.4)^{3}}+\frac{0.130518972}{(0.4)^{5}}\right|$$
$$<(0.001)\cdot980m \quad (5)$$

which results in our choice $\alpha=1.25\times10^{-10}$ (Greenspan, 1989), where the number 980 is the acceleration of gravity. The dynamical equation for the motion of each quasimolecule is

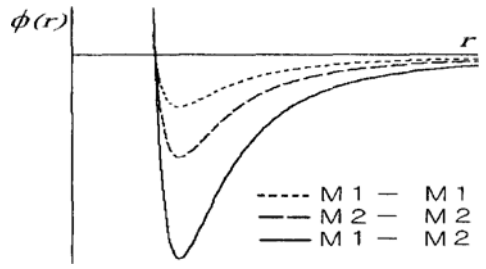

Fig. 2 Potential function for composite.

$$m\frac{d^{2}\boldsymbol{R}_{i}}{dt^{2}}=(1.25\times10^{-10})\sum\left[\left(-\frac{3.262974315}{(R_{ij})^{3}}+\frac{0.130518972}{(R_{ij})^{5}}\right)\frac{\boldsymbol{R}_{ij}}{R_{ij}}\right] \quad (6)$$

in which $\boldsymbol{R}_{i}$ is a position vector of the point P_{i}, and $\boldsymbol{R}_{ij}$ is a position vector with initial point P_{i} and terminal point P_{j}. The summation is taken over the neighbors of P_{i}. By introducing the transformation relations $R^{*}=4R$ and $T^{2}=10t^{2}$, Eq. (6) reduces to

$$\frac{d^{2}\boldsymbol{R}_{i}^{*}}{dT^{2}}=\sum\left[\left(-\frac{1.530099184}{(R_{ij}^{*})^{3}}+\frac{0.979263473}{(R_{ij}^{*})^{5}}\right)\frac{\boldsymbol{R}_{ij}^{*}}{R_{ij}^{*}}\right] \quad (7)$$

Because we wish to simulate the bending behavior of a laminar composite material with two layer, we should assume 3 potentials-a potential for material 1-material 1 bonding, a potential for material 2-material 2 bonding, and a potential for material 1-material 2 bonding as Fig. 2.

Material 1 is a soft material based on the force function of quasimolecular dynamics for pure copper. Material 2 is introduced as a fictitious hard material which has two times the strength of material 1. Based on the experimental data for other composite materials(Triantafyllidis, et al., 1982), where the interface is stronger than the substrate, these materials are assumed to be the adhesive strength of the interface, which is twice that of material 2.

Therefore, if each potential is defined, we can derive the dynamical eqnations of motion of the fictitious material as follows.

$$\frac{d^{2}\boldsymbol{R}_{i}^{*}}{dT^{2}}=\sum\left[\left(-\frac{1.5}{(R_{ij}^{*})^{3}}+\frac{1.0}{(R_{ij}^{*})^{5}}\right)\frac{R_{ij}^{*}}{\boldsymbol{R}_{ji}^{*}}\right]$$

; material 1 —material 1

$$\frac{d^2\boldsymbol{R}_i^*}{dT^2}=\Sigma\left[\left(-\frac{3.0}{(R_{ij}^*)^3}+\frac{2.0}{(R_{ij}^*)^5}\right)\frac{R_{ij}^*}{\boldsymbol{R}_{ji}^*}\right]$$
: material 2 —material 2 (8)
$$\frac{d^2\boldsymbol{R}_i^*}{dT^2}=\Sigma\left[\left(-\frac{6.0}{(R_{ij}^*)^3}+\frac{4.0}{(R_{ij}^*)^5}\right)\frac{R_{ij}^*}{\boldsymbol{R}_{ji}^*}\right]$$
: material 1 —material 2

Now, to solve Eq. (8) numerically, we adopt the leap-frog method, a kind of Verlet method which is frequently used in MD simulation. For a positive time step Δt, let $t_k=k\Delta t$, where $k=0, 1, 2\cdots\cdots$. Here, we assume that the number of particles is N. Also, at t_k let P_i having mass m_i be located at $r_{i,k}$, with velocity $v_{i,k}$, and acceleration $a_{i,k}$. Then, according to the leap-frog formulas, the position, velocity and acceleration are expressed as follows:

$$\vec{v}_{i,1/2}=\vec{v}_{i,0}+\frac{(\Delta t)}{2}\cdot\vec{F}_{i,0}/m_i \quad (9)$$
$$\vec{v}_{i,k+1/2}=\vec{v}_{i,k-1/2}+(\Delta t)\,\vec{F}_{i,k}/m_i,\quad k=1, 2, \cdots$$
$$\vec{r}_{i,k+1}=\vec{r}_{i,k}+(\Delta t)\,\vec{v}_{i,k+1/2},\quad k=0, 1, 2, \cdots$$

In order to simulate crack initiation and propagation behavior in QMD, it is necessary to break the quasimolecular bond when the force acting between two neighboring quasimolecules reaches a certain limit. In this study we introduce the separating criterion of quasimolecular bond recommended by Ashurst and Hoover(1976). There the quasimolecular bond is broken when the distance between two neighborhood quasimolecules reaches the distance R^* at which dF/dR^* first becomes negative. From Eq. (8), then, $R^*=1.05409$.

3. Numerical Simulation Models

The size of the specimen is 8cm×19. 9186cm, which gives an aspect ratio of 1:2. 5. In the simulation of bending fracture we use a laminar composite of two layers(material 1 and material 2) with a thickness ratio of 1/3. To clarify the effect of the existence and position of the hard material layer of the composite material, we simulated 3 model cases and compared their results. Model I is the case of a homogeneous specimen of soft material 1. Model II is the case of a composite specimen with hard material 2 at the outer surface and soft material 1 at the inner surface. Model III is the opposite of Model II.

In order to generate naturally the crack initiation and propagation at the area under excessive tensile stress, a geometrical imperfection of the specimen is introduced as a V-notch shape on the upper convex surface of the specimen as shown in Fig. 3.

As a boundary condition of uniform bending, a constant-displacement was applied to both ends. During uniform bending simulation, the arc length of the neutral axis of the specimen is kept at a constant value, and the quasimolecules of both ends are assigned to turn by a unit degree per unit time as shown in Fig. 4.

As a boundary condition to simulate bending deformation, at each increment of the simulation the new positions of the quasimolecules at both ends are given by(Kim and Park, 1998)

$$\begin{bmatrix}X'\\Y'\end{bmatrix}=\boldsymbol{Q}\begin{bmatrix}X\\Y\end{bmatrix}-\boldsymbol{D}$$
$$=\begin{bmatrix}\sin\Delta\theta & \cos\Delta\theta\\ \cos\Delta\theta & -\sin\Delta\theta\end{bmatrix}\begin{bmatrix}X\\Y\end{bmatrix} \quad (10)$$

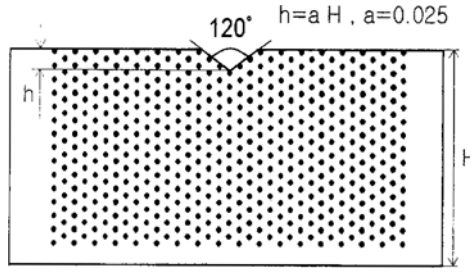

Fig. 3 The initial imperfection of the specimen introduced on the upper convex surface.

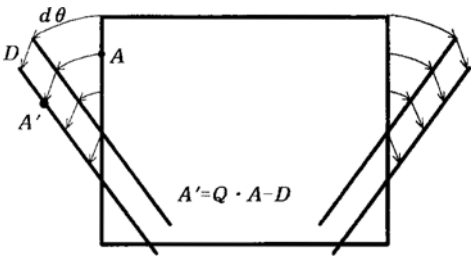

Fig. 4 Displacement boundary condition of quasimolecule at both ends.

$$-\begin{bmatrix} l-\frac{l}{\Delta\theta}\cdot\sin\Delta\theta \\ \frac{l}{\Delta\theta}-\frac{l}{\Delta\theta}\cdot\cos\Delta\theta \end{bmatrix}$$

where l is the half length of the neutral line. The Q matrix represents the rotation transformation of the coordinate axis, and the D matrix is introduced to take into consideration the fact that the neutral line of the specimen has a curvature proportion al to the turning angle. The turning angle θ is measured from the vertical line to the quasimolecules on the end line. The time step ΔT is taken as 0.1 and the turning step $\Delta\theta$ is kept at 0.01. So, $\Delta\theta/dT=0.1$ (deg/time).

4. Numerical Results and Discussion

First, the general features of bending deformation of homogeneous materials were studied in order to clarify the effect of the existence and the position of a hard material layer on the bending fracture behavior. Figures 5, 6 and 7 show the deformation behaviors and crack propagation tendency during bending for the homogeneous material, model I case. Homogeneous material, the figures correspond to turning angles of $\theta=17°$, 18° and 22°, respectively. Until bending angle of $\theta=17°$ (Fig. 5), the specimen seems to deform uniformly with pure bending, in which generally the upper convex surface is under tensile stress and the lower concave surface under compressive stress. However, when the turning angle reaches $\theta=18°$ (Fig. 6), a visible crack from the notch occurs due to the high tensile stress acting on the upper convex surface, at which the bond of quasimolecules is first broken. The crack generated from the notch propagates deep in the specimen as the specimen continues to bend. In this figure, the crack propagated asymmetrically into two directions. It seems to result from the fact that the number of left side quasimolecules (2347) is smaller than that of right side quasimolecules (2348; The rest 3 is eliminated as the notch). Strictly speaking, this means the specimen is slightly asymmetric.

Figure 7 for the deformed state of $\theta=22°$ illustrates that the crack propagation extends deeply into the center of the specimen, and another crack propagates from the inclined direction to the vertical line. Especially at the concave surface of the specimen, a compressive bifurcation is induced by extruding some quasimolecules outward on which a compressive force acts. Also the occurrence of the compressive bifurcation on the concave surface seems to decrease the crack propagation velocity. This tendency is supported by the experimental results on actual materials everywhere(Triantafyllidis, et al, 1982).

Figures 8, 9 and 10 illustrate the longitudinal force distributions, F_X, interacting between two neighborhood quasimolecules along the y-axis positions of the quasimolecules for $\theta=17°$, $\theta=18°$ and 22°, respectively. The measurement of the interacting forces was performed at the vicinity of the notch area because of the stress propagation

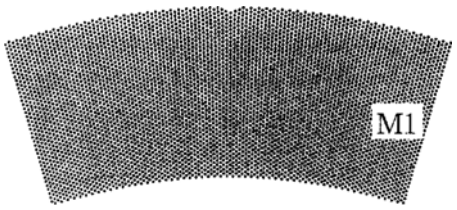

Fig. 5 Deformed shape at turning angle. $\theta=17°$ (Model I)

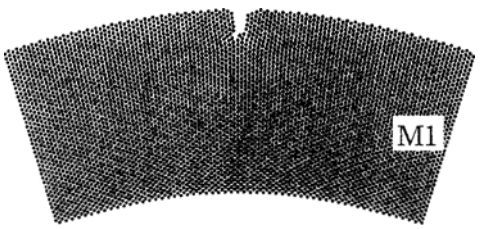

Fig. 6 Deformed shape at turning angle. $\theta=18°$ (Model I)

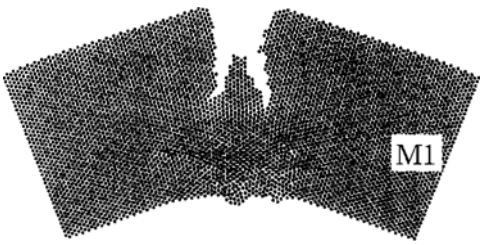

Fig. 7 Deformed shape at turning angle. $\theta=22°$ (Model I)

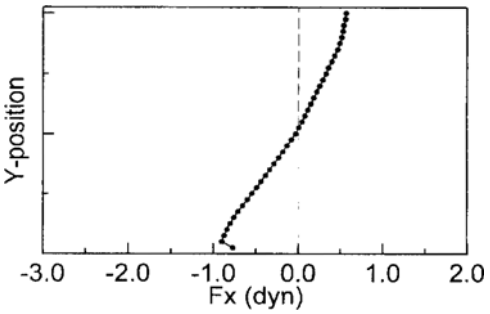

Fig. 8 The force distribution along y axis position of $\theta=17°$ for model I.

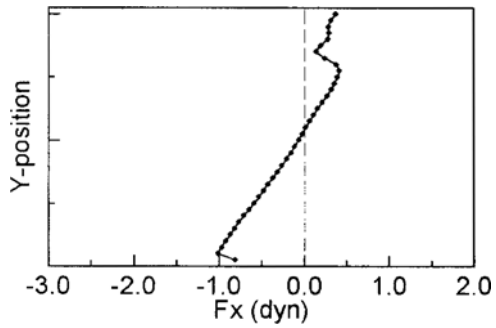

Fig. 9 The force distribution along y axis position of $\theta=18°$ for model I

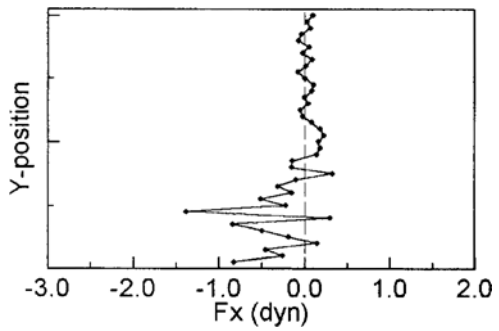

Fig. 10 The force distribution along y axis position at $\theta=22°$ for model I.

velocity. Here, the forces at the quasimolecules locating between the 2755th and the 2794th molecules along the AA cross-section as marked in Fig. 11 are measured. In the case of Fig. 8, for a bending angle of $\theta=17°$, the longitudinal forces of each quasimolecule are distributed almost uniformly in proportion to the y-distance of each quasimolecule from the neutral axis, center line of the specimen. This assures that uniform bending deformation is preserved until $\theta=17°$ as discussed above. But, in Fig. 9 at $\theta=18°$, the proportional distribution of longitudinal force is first broken, and the force acting at the upper convex surface diminishes to zero. The area where the force approaches zero becomes wider as the specimen bends more as shown in Fig. 10 of $\theta=22°$.

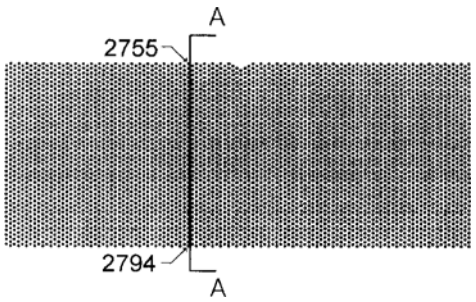

Fig. 11 The initial state of specimen with V-notch before bending.

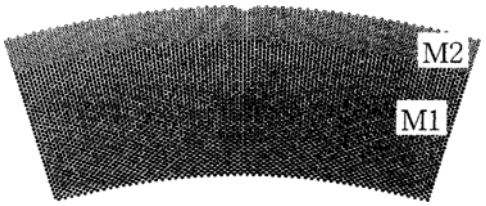

Fig. 12 Deformed shape at $\theta=17°$(Model II).

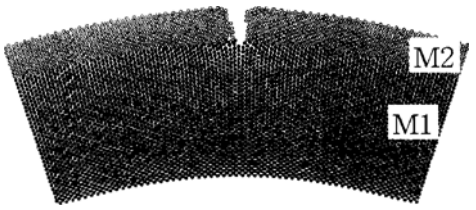

Fig. 13 Deformed shape at $\theta=18°$(Model II).

Figures 12~17 show the deformed states and the force distribution at $\theta=17°$, 18° and $\theta=20°$ for the model II specimen, where the outer material has a higher strength than the inner material. Until the specimen bends to $\theta=17°$ (Fig. 12), the specimen seems to deform uniformly with pure bending, in which generally the upper convex surface is under tensile stress and the lower concave surface under compressive stress like the homogeneous case of model I. However, the crack propagation extends to the interface of the specimen in Fig. 13. Fig. 14 showing the deformed state at $\theta=20°$ illustrates

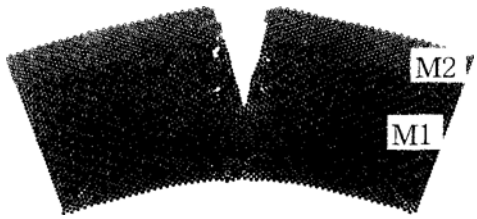

Fig. 14 Deformed shape at $\theta=20°$ (Model II).

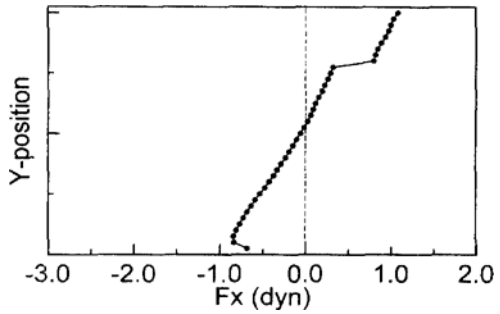

Fig. 15 The force distribution along y axis position at $\theta=17°$ for model II.

that the crack propagation extends deep into the center of the specimen. Also comparing with the model I case, the crack for model II propagates rapidly into the specimen. As shown in the Fig. 14, we can see many voids that occur naturally around both sides of the fractured surface. The number of voids is increased in conformity with the bending deformation. It can be deduced from the fact that the neutral axis of the model II case moves in the upward direction because of the existence of high strength material on the upper side. We can also find a compressive bifurcation at the lower concave surface of the specimen.

Figure 15 shows the force distributions along the y-axis of quasimolecules for the bending angle of $\theta=17°$. There the longitudinal forces of each quasimolecule are distributed almost uniformly in proportion to the y-distance of each quasimolecule from the neutral axis (center line of the specimen). In this figure, the stepped increment of the longitudinal force shown at the boundary of two materials seems to be generated due to the difference in material strength between both sides. This result matches well with other experiments or theories for laminar composite

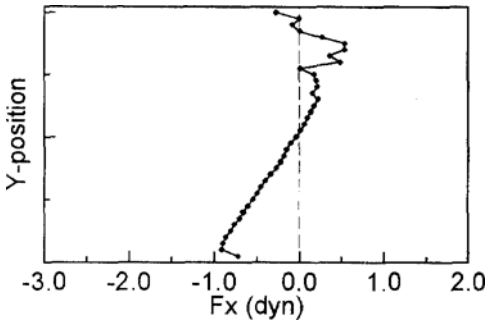

Fig. 16 The force distribution along y axis position at $\theta=18°$ for model II.

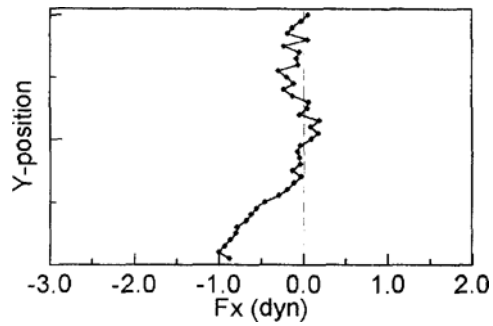

Fig. 17 The force distribution along y axis position at $\theta=20°$ for model II.

material (Lee, 1993; Yoshida, et al., 1998).

Figures 16 and 17 also correspon to $\theta=18°$ and 20° respectively. In Figure 17 at $\theta=20°$, as can be expected, the zero force region becomes wider even though the proportional distribution is maintained relatively well at the compressive region.

Figures 18~21 show the deformed states and the force distributions at $\theta=15°$ and $\theta=17°$ for the model III specimen, which is the opposite case of the model II. Comparing with Fig. 6 of the model I case, Fig. 18 for the deformed state of $\theta=15°$ shows that the crack occurs earlier than the model I case. It seems to stem from the fact that the higher tensile stress acts on the convex surface, because the neutral axis moves toward the bottom due to the existence of a high strength inner material. However, the pattern of crack propagation is very similar with model II except no that there are voids around the fractured surface. As can be expected, the fracture

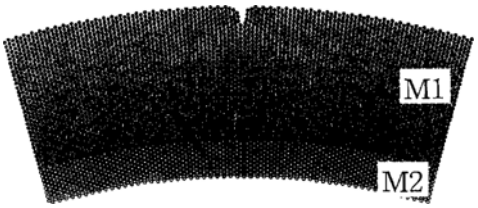

Fig. 18 Deformed shape at $\theta=15°$(Model III).

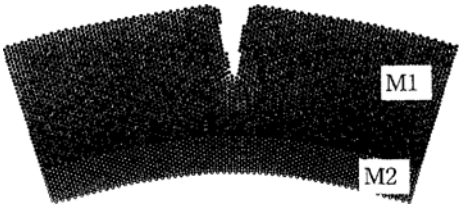

Fig. 19 Deformed shape at $\theta=17°$(Model III).

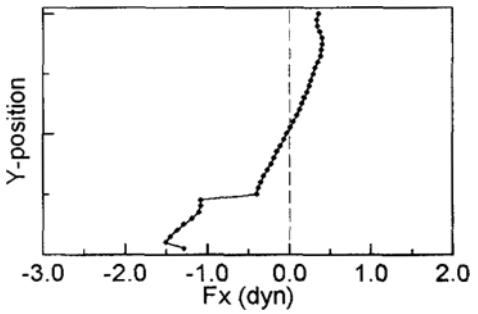

Fig. 20 The force distribution along y axis position at $\theta=15°$ for model III.

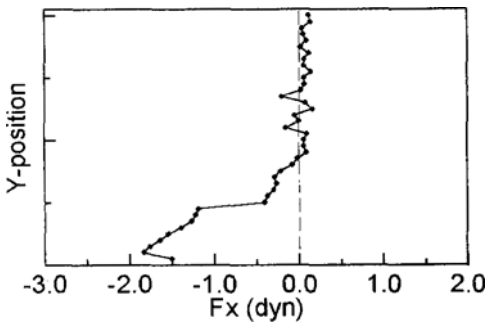

Fig. 21 The force distribution along y axis position at $\theta=17°$ for model III.

extends deeply at $\theta=17°$ in Fig. 19. But, unlike Fig. 14, the compressive bifurcation hardly appears on the concave side of specimen. Figure 20 shows that the proportional distribution of the longitudinal forces is maintained except at the upper area of the notch site where the debonding of quasimolecules is generated. In Fig. 21, at $\theta=17°$ the region where the force approaches zero due to the debonding of quasimolecules becomes wider.

5. Conclusion

According to quasimolecular dynamic simulations for bending deformation of laminar composites we were able to verify fracture behavior, the occurrence of voids, and the crack propagation pattern of the composite material. Comparing to the Model I case, the bending crack propagation for the Model II case composite material occurs as bending progresses, and many voids near the cracked surface are generated. In the Model III case, bending fracture occurs earlier than the Model I case. However, the compressive bifurcation seems hardly to appear on the bottom surface of the hard material. Therefore we can conclude that if a composite material with notch is subjected to uniform bending, the most dangerous case for bending fracture is the Model III case. Moreover, according to the position of the hard material in the composite material under bending deformation, the magnitude of the bending angle to initiate the fracture at the crack tip was varied significantly. This reason may be attributed to the movement of the neutral line of the composite specimen. We leave for futher study this movement of the neutral line.

References

deCelis, B., Argon, A. S., and Yip S., 1983, "Molecular Dynamics Simulation of Crack Tip Processes in Alpha-Iron and Copper," *J. Appl. Phys.* , Vol. 54, pp. 4864~4878.

Kitagawa, H., Nakatani, A., and Shibutani, Y., 1993, "Study on Computational Modelling for Materials with Crystalline Structure," *Trans. JSME,* Vol. A59., pp. 1834~1841. (in Japan)

Greenspan, D., 1986, "Quasi-Molecular, Particle Modeling of Crack Generation and Fracture," *Computers and Structures,* Vol. 22, pp. 1055

~1061.

Greenspan, D., 1989, "Supercomputer Simulation of Cracks and Fractures by Quasimolecular Dynamics," *J. Phys. Chem. Solids.*, Vol. 50, pp. 1245~1249.

Kim, Y. and Park, J., 1997, "Analysis of Metallic Solid Fracture by Quasimolecular Dynamic," *Advanced Method in Materials Processing Defects, M. Predeleanu and G. Gilormini ed.*. Elsevier, pp. 457~458

Maiti, D. K. and Sinha, P. K., 1996, "Bending, Free Vibration and Impact Response of Thick Laminated Composite Plates," *Comp. Struct.*, Vol 59, No 1, pp. 115~129.

Suga, M., Honda, M., Nagae, M., Seki, M., Izawa, T., and Kaneko, Y., 1989, "The Newly Developed Stainless Clad Steel Plates for the Hull Structure of Chemical Tankers," *NKK Tech. Review*, Vol. 55, pp. 55~72.

Triantafyllidis, N., Needleman, A., and Tvergaard, V., 1982, "On the Development of Shear Bands in Pure Bending," *Int. J. Solids Structures*, Vol. 18. No. 2, pp. 121-138.

Yoshida, F., Okada, T., Itoh, M., Harada, Y., and Ohmor, M., 1998, "Bendability of Aluminium and Steel Clad Chromium Plates," *Metals and Materials*, Vol. 4, No. 3, pp. 426~431.

Ashurst, W. T. and Hoover, W. G., 1976, "Microscopic Fracture Studies in the Two -Dimensional Trianglar Lattice," *Physical Review*, B14, pp. 1465~1473.

Kim, Y. and Park, J., 1998, "Molecular Dynamics Simulation for Micro Fracture Behavior of Material," *KSME Int. J.*,. Vol. 12, No. 3, pp. 388~395.

Lee, D., 1993, Mechanics and Manufacturing Process of Composite Material, Sung-an-dang press, Korea, Seoul (in Korea).